

THE KINETICS OF HCO_3^- SYNTHESIS RELATED TO FLUID SECRETION, pH CONTROL, AND CO_2 ELIMINATION

Thomas H. Maren

Department of Pharmacology and Therapeutics, University of Florida College of Medicine, Gainesville, Florida 32610

INTRODUCTION

In 1928 Henriques (20) deduced from the rates of $\text{HCO}_3^- \rightleftharpoons \text{CO}_2$ reactions published by Faurholt (14), that the conversion process was too slow to account for the loss of respiratory CO_2 across the lung. Henriques sought for an enzyme in blood to catalyze the process; for reasons I have reviewed elsewhere (32) he concluded that there was none, but that the rapid reaction was mediated by carbaminohemoglobin (20). Meldrum & Roughton, five years later, discovered carbonic anhydrase (CA) in red cells (38). It is now clear that the interconversion of $\text{CO}_2 \rightleftharpoons \text{HCO}_3^-$ has physiological implications far greater than the carriage and excretion of metabolic CO_2 in red cells. This process occurs in other sites, and the reaction is also central to the formation of H^+ and HCO_3^- in secretory organs (reviewed in 30).

In the present chapter I consider anew HCO_3^- formation in certain secretory processes, in generation of an alkaline milieu, and in subserving the excretion or removal of CO_2 from certain special tissues. Chemically, these are analogous to the interconversion in red cells; the latter is considered by Klocke elsewhere (this volume). An earlier review (34) covers other aspects of HCO_3^- or CO_3^{2-} synthesis, i.e. in shell formation and salivary secretion.

The purpose of this review is to try to coordinate this subject by weaving

together those elements that allow for coherent conclusions. In my view this is quite possible and can be stated in a single sentence: HCO_3^- synthesis plays a role in fluid formation as a gegen ion for sodium transport or for chloride exchange, and as a carrier for CO_2 , and as a pH regulator in metabolism.

Until recently HCO_3^- has been the forgotten ion of physiology and membrane electrophysiology. If we use an analogy with Cl^- , we find at once that while the distribution $\text{Cl}_{\text{in}}/\text{Cl}_{\text{out}} \cong 0.1$, when inserted into the Nernst equation, corresponds to the usual transmembrane potential of -60 mV, the distribution for HCO_3^- does not, since $\text{HCO}_3^-_{\text{in}}/\text{HCO}_3^-_{\text{out}} = 10 \text{ mM}/25 \text{ mM} = 0.4$, yielding -24 mV. What is the reason for this, since there is no evidence that HCO_3^- is less permeant than Cl^- ? Almost certainly this is because HCO_3^- is formed continuously within the cell, raising $\text{HCO}_3^-_{\text{in}}$.

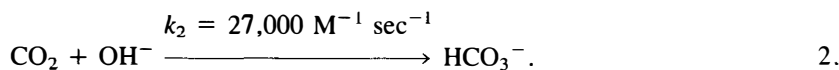
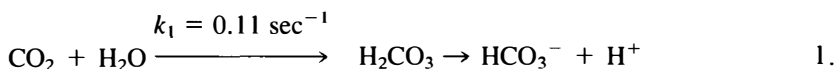
Although the chemical and pharmacological evidence is convincing that HCO_3^- synthesis occurs, there is far less evidence to connect this with transmembrane transport. Even when HCO_3^- transport is discussed, and the effect of CA inhibitors documented, the fact of ion synthesis is rarely mentioned. A brilliant series of experiments initiated by Frömter is given as an introduction, since they demonstrate these important relations (4, 6).

Transmembrane potential difference (P.D.) from cell to peritubular capillaries was measured in rat kidneys in situ, (normally 74 mV) under conditions of changing peritubular HCO_3^- concentration and inhibition of CA. When peritubular (but not luminal) HCO_3^- was lowered to 3 mM, the P.D. fell about 35 mV. This depolarization is reduced to 15 mV when a CA inhibitor is added to the peritubular perfusate or blood. The drug effect was localized to the enzyme at or in the peritubular membrane (5). Thus, lowering $\text{HCO}_3^-_{\text{out}}$ decreases P.D., but when the formation of $\text{HCO}_3^-_{\text{in}}$ is reduced by CA inhibition, the effect of reducing $\text{HCO}_3^-_{\text{out}}$ is muted, since now both $\text{HCO}_3^-_{\text{out}}$ and $\text{HCO}_3^-_{\text{in}}$ are lowered. The P.D. always favors HCO_3^- exit, even from low intracellular concentration. This type of experiment also was done by reducing pericapillary sodium. This depolarizes the membrane as does reduction of HCO_3^- (45, 67). The circle closes by the finding that acetazolamide inhibits Na^+ movement. This shows that Na^+ movement is driven by the HCO_3^- gradient (18). A recent short publication reviews the matter and emphasizes that the stoichiometry is 3 HCO_3^- :1 Na^+ (53) and that Cl^- manipulation has no effect. This evidence suggests a rheogenic Na^+ - HCO_3^- transport, dependent in part on HCO_3^- synthesis from CO_2 .

Although the equivalent experiments have not been done with pancreas, choroid plexus, or ciliary processes, partly because of technical problems, it is evident that the data available imply the same synthesis-transport processes as of the Frömter model for renal HCO_3^- reabsorption.

CHEMISTRY OF HCO₃⁻ SYNTHESIS*Uncatalyzed*

There are two routes to the formation of HCO₃⁻ from CO₂: hydration and hydroxylation, each with rate constants k_1 and k_2 given below for 37°C (44):¹



Reaction 1 is independent of pH, while Reaction 2 obviously is pH dependent. By converting Reaction 2 to pseudo first-order at fixed pH, we may judge the relations between the two reactions. At pH 7, k_2 yields $27,000 \text{ M}^{-1} \text{ sec}^{-1} \times 10^{-7} \text{ M} = 0.0027 \text{ sec}^{-1}$, which is small compared to k_1 . At pH 9, however, the value is 0.27 sec^{-1} and Reaction 2 dominates. This will be used for the physiological model.

I will develop the idea that the driving force in physiological HCO₃⁻ formation is the OH⁻ gradient. This makes it unnecessary to invoke a back reaction, since presumably the pH at the site of HCO₃⁻ formation is considerably higher than the pH in the final fluid.

Catalyzed

There are multiple CAs, but in secretory cells we are concerned with enzyme II, also known as C. The membrane-bound enzymes, IV, is not completely characterized, and its kinetic properties are akin to II. For II, the hydration turnover number (k_{cat}) at 37° is $1.3 \times 10^6 \text{ sec}^{-1}$ and $K_m = 13 \text{ mM}$ (44). We derive the relation between the uncatalyzed rate (or rate constant) and the catalyzed as follows:

$$V_{\text{cat}} = (k_{\text{cat}} \cdot E \cdot \text{CO}_2) / (K_m + \text{CO}_2), \quad 3.$$

where E is the enzyme concentration. Since $K_m > \text{CO}_2$ in physiological systems, CO₂ may be neglected in the denominator, and

$$V_{\text{cat}} = k_{\text{cat}} / K_m \cdot E \cdot \text{CO}_2 = 10^8 \text{ sec M}^{-1} \cdot E \cdot \text{CO}_2. \quad 4.$$

To obtain a practical "first-order catalytic rate constant" (denoted k_{pcat}) we omit the substrate and insert the value of E into Equation 4. Thus if E is 10^{-6}

¹ k_2 has not been measured accurately at 37°. The 25° value is $8500 \text{ M}^{-1} \text{ sec}^{-1}$ (51). The ratio of k_1 values at 37°/25° is 0.11/0.035 (44). Assuming the same for k_2 , we arrive at $27,000 \text{ M}^{-1} \text{ sec}^{-1}$.

M, $k_{\text{pcat}} = 100 \cdot \text{sec}^{-1}$ and $V_{\text{cat}} = k_{\text{pcat}} \cdot \text{CO}_2$. For the usual CO_2 concentration in tissues (1 mM), $V_{\text{cat}} = 100 \text{ mM sec}^{-1}$.

The term k_{pcat} is directly comparable to k_1 or k_2 (in its pseudo first-order form), the uncatalyzed rate constants. In the above example (in which E is the only variable) the k_{pcat} is about 400 times greater than the uncatalyzed rate constant calculated above for pH 9.² The range of E in the cytoplasm of secretory tissues is $0.3 \mu\text{M}$ (ciliary processes) to $22 \mu\text{M}$ [choroid plexus (30, 60)].

HCO_3^- SYNTHESIS IN ION AND FLUID MOVEMENT; RATES IN RELATION TO THE CHEMICAL PROCESSES

In this section I will show that HCO_3^- movement is controlled by its synthesis from CO_2 , and that H_2O , HCO_3^- and Na^+ move together in pancreatic juice (PJ), aqueous humor (AH), and cerebrospinal fluid (CSF).³ The alligator kidney, in which HCO_3^- formation subserves Cl^- exchange also, is considered.

The reactions within the cell are conceived as having two parts, the protolysis of water and the hydroxylation of CO_2 ,



The metabolic path must be similar, if not identical, to that now accepted for the coupling of oxidative metabolism to proton pumps (39). Both constructs demand that the membranes performing these functions be assymetrically disposed in the cell, with vectorial properties, i.e. protons and electrons accumulate on opposite faces acting as cathode and anode. It has been shown that Reactions 2 and 5 above are separable, i.e. one can have acidification (59) or (presumably) alkalization without CO_2 . When the numbers shown below are considered, it will be evident that the uncatalyzed formation of HCO_3^- could not have a measurable rate if $[\text{OH}^-] = 10^{-7}$ or even 10^{-6} M. Yet there is a significant uncatalyzed process, indicated by the residual rates after inhibition of CA. On the other hand, if $[\text{OH}^-] = 10^{-4}$, the reaction would be so rapid that an enzyme would not be necessary. Indeed, the effect of an inhibitor would not be apparent since the rate dependent on Reaction 2

²Since the catalytic rate is maximal at pH 8–9 (24), this comparison appears valid.

³There are other instances of HCO_3^- formation not as well studied as the present examples (34). The 1987 Annual Review of Physiology (Vol. 49) has a section on gastrointestinal physiology giving some data on HCO_3^- output in duodenum and colon, and reabsorption in gall bladder. There are also chapters on pancreas and parietal cell pH.

would exceed the physiological rate. Thus, for the purpose of calculation, and so that we are not held up in our thinking by this detail, however important, we use 10^{-5} M as the OH⁻ concentration in the anatomically undefined secretory volume. This yields (see above) $k_2 \cdot (\text{OH}^-)$ for Equation 2 of 0.27 sec^{-1} . The uncatalyzed rate (V_{unc}) is for pH 9 and physiological P_{CO_2} :

$$\begin{aligned} V_{\text{unc}} &= k_2 (\text{OH}^-) (\text{CO}_2) = 0.27 \text{ sec}^{-1} \cdot 10^{-3} \text{ M} \cdot 10^{-3} \text{ L} \\ &= 16 \mu\text{mole min}^{-1} \text{ for 1 ml of reaction volume.} \end{aligned} \quad 6.$$

The reaction volume, at the present time, must be but an approximation. This will be given, along with its basis, in each physiological example.

The catalytic rate is given by Equation 4, as follows:

$$\begin{aligned} V_{\text{cat}} &= 10^8 \text{ sec M}^{-1} \cdot E \cdot 10^{-3} \text{ M} \\ &= 60 \times 10^5 \text{ min}^{-1} \cdot E. \end{aligned} \quad 7.$$

For a cell reaction volume of 1 ml as used above for V_{uncat} , E may be used in units of $10^{-3} \mu\text{mole ml}^{-1}$. Thus, as in the example in the introduction where E is 10^{-6} M or $1 \mu\text{mole L}^{-1}$ cell volume,

$$V_{\text{cat}} = 6000 \mu\text{moles min}^{-1} \text{ per ml or } 100 \text{ mM sec}^{-1}. \quad 8.$$

Note that this exceeds V_{unc} by 360-fold. It is shown below that this calculated catalytic rate also greatly exceeds the observed physiological rate. The actual value of V_{cat} is not of great interest since it is so far above the biological rate.

Pancreas

The overt appearance of HCO₃⁻ in PJ turned attention early to the role of CO₂ and CA (reviewed in 30). A broad and excellent review on HCO₃⁻ secretion by pancreatic duct cells, emphasizing mechanisms and control, recently appeared (8). The enzyme has been localized in the duct and centroacinar cells, in both cytoplasm and membranes. There was weak cytoplasmic staining in acinar cells (3).

I review two papers which give full data on electrolyte excretion following CA inhibition and alteration in acid-base balance in two species in vivo. The isolated in vitro rabbit pancreas appears less suitable for analysis because of very low secretory rates (26, 27).

Table 1 shows data from dog (42) and pig (41) following secretin in full dose, 2–3 units kg⁻¹. When CA is inhibited (Col. 2, Rows 1–2 and 6–7), the rates of HCO₃ and fluid output (V_{inh}) drop to roughly the same degree in each species (47% in dog and 33% in pig). This illustrates a most important principle: HCO₃⁻ formation and fluid output are linked. This will recur in all other organs studies.

Is V_{inh} the uncatalyzed rate of HCO_3^- formation, or is some other process involved, i.e. active secretion of HCO_3^- ? We approach this by calculating the uncatalyzed rate, as in Equation 6 above, which yields that V_{unc} is $16\text{ }\mu\text{moles min}^{-1}$ for each ml of secretory volume. If the volume of the ductal cells equals the volume they secrete in two minutes (8), their volume per kg body weight is 0.078 ml (dog) and 0.150 ml (pig), from which we calculate $V_{unc} = 1.3\text{ }\mu\text{mole min}^{-1}$ for dog and $2.4\text{ }\mu\text{mol min}^{-1}$ for pig (Col. 4). These are remarkably close to the observed V_{inh} (Col. 2, Rows 1 and 6) in view of the guess at the pH (see above). We tentatively conclude that HCO_3^- formation in pancreas is carried out entirely by the hydroxylation of CO_2 , uncatalyzed and catalyzed.

The chemically calculated enzyme rate is obtained from Equation 7 after entering the secretory volume (0.078 ml in dog) and the enzyme concentration E. We obtained $0.34\text{ }\mu\text{mol kg}^{-1}$ for the whole dog pancreas; using the estimate (8) that the secretory cells have but 4% of gland cell mass, we may

Table 1 Pancreatic HCO_3^- excretion in dog (42) and pig (41) following secretion

	Micromoles $HCO_3^- \text{ min}^{-1}$ per kg body weight			
	1 ^a $V_{obs} = V_{total}$	2 ^b $V_{inh} = V_{unc}$	3 ^c V_{enz} (Col. 1 – Col. 2)	4 ^d Calc. V_{unc}
<u>Dog</u>				
1 Normal	4.3	2.1	2.2	1.3
2 (Flow, normal $\mu\text{L min}^{-1} \cdot \text{kg}^{-1}$)	39	19	20)	
3 HCl	1.8	0.8	1.0	0.6
4 $NaHCO_3$	5.9	3.6	2.3	2.6
5 CO_2	4.6	2.7	1.9	1.3
<u>Pig</u>				
6 Normal	12	4	8	2.4
7 (Flow, normal $\mu\text{L min}^{-1} \cdot \text{kg}^{-1}$)	75	26	49)	
8 HCl	6	3	3	
9 $NaHCO_3$	16	3	13	

^a $V_{obs} = V_{total}$ is the normal rate in vivo.
^b $V_{inh} = V_{unc}$ is the observed rate in vivo after full carbonic anhydrase inhibition, presumed to represent the uncatalyzed rate of HCO_3^- formation (see text).
^c V_{enz} = the enzymic rate of HCO_3^- formation in vivo.
^dCalc. V_{unc} = the uncatalyzed rate calculated from chemical rate constants (see text).

use 8.5 $\mu\text{mol L}^{-1}$ for E . Entering this in Equation 7 along with the cell volume per kg we obtain through Equation 8:

$$\begin{aligned} V_{\text{cat}} &= 6000 \mu\text{moles min}^{-1} \text{ per ml} \times 8.5 \mu\text{mol L}^{-1} \times .078 \text{ ml} & 9. \\ &= 400 \mu\text{moles min}^{-1} \text{ kg}^{-1}. \end{aligned}$$

This is 100 times the total in vivo rate and 200 times the observed enzymic rate in the dog (Table 1). These numbers show the "enzyme excess" in the CA system (30) and are supported by inhibition studies as follows. The minimal dose of acetazolamide or methazolamide for complete inhibition is 5–50 mg kg⁻¹ varying with the organ system and enzyme concentration. In pancreas it is 10 mg kg⁻¹ (42). Drug concentration in pancreas at this dose is 15 μM (42); if E is 8.5 μM , free drug concentration (I_f) is 6.5 μM . The inhibition constant (K_I of acetazolamide is 0.01 μM , so that fractional inhibition of the enzyme (i) is well over 99% according to Equation 10:

$$\% \text{ inhibition} = \frac{I_f}{K_I + I_f} \times 100 = 99.84, \quad 10.$$

where I_f is the concentration of free inhibitor. This independent estimate agrees well with the enzyme excess calculated on kinetic grounds.

Table 1 (Col. 1, Rows 3 and 8) shows that metabolic acidosis decreases PJ HCO₃⁻ output and fluid flow. Rows 4 and 8 show that metabolic alkalosis increases these functions. The same effect is seen in the isolated perfused cat pancreas (1a). These findings are consistent with the idea that the cellular OH⁻ gradient plays a role in secretion. Specifically, in metabolic acidosis plasma OH⁻ is decreased by about 2-fold, and in metabolic alkalosis it increased the same degree. P_{CO₂} is nearly unaffected (42). If these changes are reflected in the cell, the calculation through Equation 6 yields the data of Col. 4 for V_{unc} . These agree pretty well with the observed V_{unc} shown in Col. 2, so it appears that variations in OH⁻ affect the uncatalyzed rate, as predicted by Equation 6.

Do variations in OH⁻ affect V_{enz} ? Theoretically they should not, since the turnover number of the enzyme is so great compared with observed rates, that small changes in substrate should have no effect. This is the case for metabolic alkalosis, compare in Col. 3, Row 1 with Row 4 and Row 6 with Row 9. However, in acidosis the enzyme rate is lowered (Col. 3, Rows 3 and 8); possibly the HCO₃⁻ is formed catalytically at usual rate but dissipated by acidotic milieu.⁴

⁴The effects of metabolic acidosis and alkalosis on HCO₃⁻ output in the secretin (or pancreozymin) stimulated in situ dog pancreas were the same as shown in Table 1. Surprisingly, however, HCO₃⁻ output provoked by dopamine was unresponsive to acid or base infusion (20a).

In respiratory acidosis, data are not substantially different from controls (Table 1, Row 1 and Row 5). This follows from Equation 6 since OH^- and CO_2 vary in opposite directions, and V_{unc} should be unchanged. V_{enz} is also unchanged. The same was found in the isolated cat pancreas (1a), but authors interpret this as showing that secretion was independent of blood pH, not realizing that the rise in P_{CO_2} matches the fall in OH^- during respiratory acidosis.

A crucial study supporting the main thesis in this review, that HCO_3^- is formed in the cell by $\text{OH}^- + \text{CO}_2$, was performed by perfusing the rabbit pancreas in vitro with solutions of various anions. HCO_3^- enhanced PJ and HCO_3^- output, and the effect was reduced by acetazolamide. However, infused acetate (or its homologues with one, three, or four carbon atoms) again enhanced secretion of PJ, but acetazolamide had no effect. The secretion was regarded as originating with basolateral H^+ efflux (in exchange for Na^+) and thus resulting in apical OH^- formation. The process was not specific for HCO_3^- (57) but extends to the other anions mentioned (and also to sulfamerazine) (47). Since these are not synthesized or involved in the $\text{CO}_2 + \text{OH}^-$ reaction, CA is not involved.

The major driving force for HCO_3^- secretion is the P.D. at the luminal membrane (-55 to -80 mV) which allows the ion to move down its electrochemical gradient when the cell concentration is about one tenth of that in the lumen. Notably, secretin (along with theophylline and cyclic AMP) lowers this P.D. (48) and the transepithelial potential (64), which is to be expected if secretin increases cellular HCO_3^- .

In summary (Figure 1A): (1.) Pancreatic duct cells are capable of producing high OH^- concentrations destined for secretion, which are then buffered by CO_2 . The P.D. favors accumulation of HCO_3^- in the lumen. This must be matched by H^+ transported to blood. Secretin elicits this process in some species (cat, dog, pig, man) but not in others (rabbit, guinea pig) (8). In some species, cholecystokinin also induces HCO_3^- output. Secretin appears to act via cyclic AMP. The mechanism behind these actions is unknown, but will be of great importance when discovered (8). (2.) Although the normal mechanism involves CA through the reaction $\text{CO}_2 + \text{OH}^- \rightarrow \text{HCO}_3^-$, this is not part of the fundamental process of H^+ - OH^- separation, since the secretory system works when other anions (cf acetate) are supplied. In this case CA inhibitors have no effect (57). (3.) Fluid movement and HCO_3^- formation are linked (here and below) in a way that has not been explained. Notably, when other anions are substituted for HCO_3^- in perfusates, fluid movement drops, usually by more than 50% (26, 27). (4.) Na^+ and HCO_3^- movement are linked in these systems as in others (Figure 1). Are they linked by a secondary active transport process ($\text{Na}^+ - 2\text{HCO}_3^- - \text{Cl}$) (See Ref. 8 for consideration of several models)? Or is there a direct chemical link between Na^+ and total CO_2 , with transported species NaHCO_3 or NaCO_3^- ?

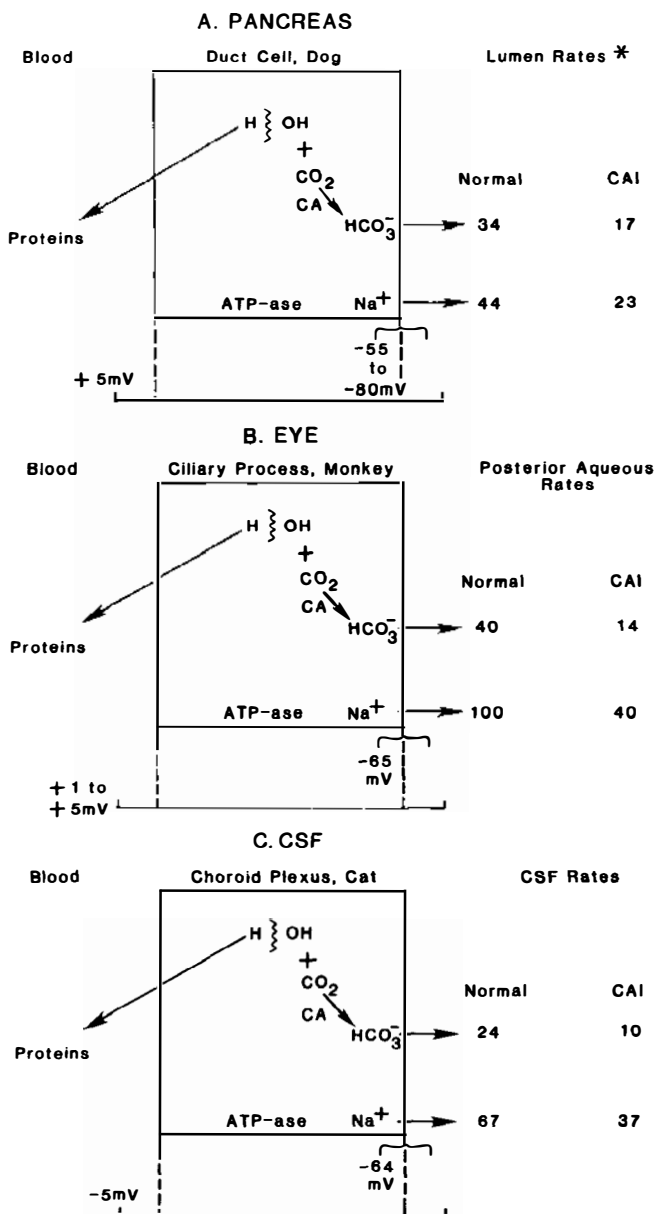


Figure 1 Rates are $\mu\text{mol min}^{-1}$ per gram or per ml volume secretory tissue. CA = Carbonic anhydrase; CAI = Complete carbonic anhydrase inhibition in vivo. Catalytic rates are the differences between total observed rates (normal) for HCO_3^- and Na^+ minus rates during CAI. Note that the rates are surprisingly similar in these three tissues despite widely different concentration of CA (see text). This shows that the enzyme concentration is not the rate-limiting feature of secretion. Cell structure or sites of enzyme activity are not implied. Data are from Tables 1-3, also Table 10 in Ref. 34. Potentials are from Ref. 48 (Pancreas), Refs. 19 and 25 (Eye), and Ref. 12 (CSF).

Eye

In the eye there are two (possibly three) tissues that produce HCO_3^- from CO_2 , catalyzed by CA. The first is the ciliary process, which produces AH. The second is the corneal endothelium, which pumps fluid out of the corneal stroma into the aqueous insuring clarity of the tissue. The third, and quite problematic, is the retina, where CA in Muller cells may have a secretory role.

In this chapter, I consider the the ciliary process since only in this case are there data quantifying HCO_3^- formation, Na^+ and fluid movement, and the effect of CA inhibition. I have reviewed the history of this subject elsewhere (35). All vertebrates so far studied have CA in the ciliary process (or folds, in fish). There is good evidence that the secretory mechanism described here is common to all classes of vertebrates.

The posterior chambers of the human, cynomolgus monkey, and rabbit eyes contain about 50 μL of AH. In the rabbit, and at least in one species of fish, the dogfish *Mustelus canis*, the HCO_3^- concentration is notably higher than in plasma (rabbit 35%, fish 100%). In dog, monkey and (probably) man there is no measurable excess of HCO_3^- in the posterior aqueous; however, the kinetics of HCO_3^- accumulation in dog and monkey show that, as in rabbit, this ion is formed from CO_2 and moves with Na^+ from plasma to the posterior chamber (35). The underlying chemistry is analagous to that of the pancreas.

Table 2 shows the rate constants and accession rates of Na^+ , Cl^- , and

Table 2 The accession rates of ions from plasma to posterior aqueous in the cynomolgus monkey: Effect of carbonic anhydrase inhibition (CAI) (31)^a

		1	2	3	4
		Plasma	k_{in}^b	Accession Rate	Calc. in
		(mM)	(min^{-1})	Col. 1 \times Col. 2	New Fluid ^c
				(mM min^{-1})	(mM)
Na^+	control	152	0.017	2.7	162
	CA inhibition		0.009	1.4	168
Cl^-	control	103	0.016	1.6	96 ^d
	CA inhibition		0.012	1.2	144
HCO_3^-	control	20	0.054	1.1	66 ^d
	CA inhibition		0.019	0.4	48

^a50 mg/kg acetazolamide i.v. given 1 hour before injections of isotope.
^bRate of isotope delivery to posterior aqueous \div counts in plasma.
^cColumn 3 \times volume posterior chamber (60 μL)/aqueous flow (1 $\mu\text{L min}^{-1}$), for controls. Flow 0.5 $\mu\text{L min}^{-1}$ during CAI.
^d Cl^- and HCO_3^- are 115 and 21 mM, respectively in the measured posterior chamber aqueous.

HCO₃⁻ from plasma to posterior aqueous of the monkey, as measured by the movement of the isotopes. Note that the calculated HCO₃⁻ concentration in new fluid is 3.3 times that of plasma, and 37% of the Na⁺ is accompanied by HCO₃⁻.⁵ Following full CA inhibition, Na⁺ accession drops 1.3 mM min⁻¹; HCO₃⁻ accession drops 0.7 mM min⁻¹. Cl⁻ movement is but slightly changed. The newly formed fluid has the same Na⁺ concentration as plasma (Table 2) and indeed is isoosmotic with plasma. Na⁺, Cl⁻, and HCO₃⁻ show one-way passage into AH and CSF; there is no evidence for exchange mechanisms (12).

We may calculate the HCO₃⁻ transport rates in the light of the uncatalyzed and catalyzed reactions, and the model given in Figure 1B. The total or observed rate is 40 μmoles min⁻¹ per g tissue and $V_{inh} = 14 \mu\text{mole min}^{-1} \text{ g}^{-1}$. The enzymic rate is thus $26 \mu\text{mole min}^{-1} \text{ g}^{-1}$. This assumes that V_{inh} is also V_{unc} ; that is, there is no other process for HCO₃⁻ formation (i.e. active ion transport) at work and which appears as part of V_{inh} . As we shall see, this is borne out by calculations to follow.

The calculated rates are derived from Equations 6 and 7. For V_{unc} , Equation 6 yields $V_{unc} = 16 \mu\text{mol min}^{-1}$ per ml secretory volume. Since V_{unc} is remarkably close to that observed for V_{inh} (Figure 1B), we assume that $V_{unc} = V_{inh}$. For V_{cat} , we follow Equations 3, 4, and 7 from which we obtain $V_{cat} = 6 \times 10^6 \text{ min}^{-1} \cdot E$. The latter concentration in isolated ciliary process is about $0.5 \mu\text{mol kg}^{-1}$. Entering this value in Equation 7 and for a cell volume of 1 ml, we get:

$$\begin{aligned} V_{cat} &= 6 \times 10^6 \text{ min}^{-1} \cdot 0.5 \times 10^{-6} \text{ M} \cdot 10^{-3} \text{ L} \\ &= 3000 \mu\text{moles min}^{-1} \text{ per ml cell volume.} \end{aligned} \quad 11.$$

This is about 100 times greater than the observed catalytic rate. The margin is less than usually found in secretory tissues, because of the very small concentration of enzyme present [compare pancreas (above) and choroid plexus (below)]. Still, with 100 times the amount of enzyme needed for normal secretion, it is inevitable that the dose-response curve for inhibition begins at 99% inhibition (no effect) and is complete at 99.9% (36).

The aqueous humor P.D. is slightly lightly negative to plasma (0.75 mV), and full CA inhibition reduces this to 0.5 mV (25). The data may reflect HCO₃⁻ diffusion potentials, as described below for CSF (2, 11). The P.D. at

⁵Table 2 uses the concentration of HCO₃⁻ in plasma for calculation, although the data and theory hold that the species moving is CO₂. In the calculation, 95% of the counts in plasma are considered HCO₃⁻, and 5% CO₂. If CO₂ were used for calculation, the rate constant would be 20-fold higher, but the accession rate of total carbon counts in AH (again 95% HCO₃⁻) would be the same. Table 3 shows the similar relations for CSF.

the apical membrane is -65 mV (cell negative, Figure 1B), but, as for pancreas, the effect of CA inhibition on this value has not been studied.

Na^+ movement is linked to HCO_3^- synthesis (Table 2, Figure 1B). Since Na^+ movement is essentially isotonic, fluid movement is a cardinal result of CA activity. Thus, inhibition of this enzyme reduces flow. Appropriate drugs have been in use for the treatment of glaucoma for 30 years (35). Although glaucoma is a disease of reduced outflow, the CA inhibitors, by reducing inflow, bring pressure back to normal in most cases of the disease.

Cerebrospinal Fluid (CSF)

The relations between CO_2 , CA, and CSF formation have a different history than PJ and AH. In no species is the CSF overtly alkaline, as PJ and AH, although the choroid plexus contains the enzyme and acetazolamide does decrease flow (30). The matter was not understood until it was found that CO_2 gas administered to fish greatly increases the concentration of HCO_3^- in CSF and that this effect was reduced by acetazolamide (31). The only explanation appeared to be that CSF HCO_3^- was catalytically synthesized from CO_2 , just as in PJ and AH. Using labelled HCO_3^- , Cl^- , and Na^+ , it was found that bicarbonate access was by far the most rapid; despite the very low ratio of $\text{HCO}_3^-/\text{Na}^+$ (1/35) in plasma, the accession of HCO_3^- was $\frac{1}{4}$ that of Na^+ . Table 3 shows similar experiments in the cat; HCO_3^- accession was about one third of Na^+ , i.e. 37% of Na^+ accession was matched by HCO_3^- and the rest by chloride. Na^+ accession was reduced 54% by CA inhibition. The calculated HCO_3^- concentration in newly formed fluid is much higher than in plasma (as in Table 2), even though the chemically measured concentration is the same. The threefold HCO_3^- excess in nascent CSF is reduced markedly by the CA inhibitors.⁶

Using the same treatment to calculate the theoretical rates as done above for PJ and AH, we find for the uncatalyzed rate (Equation 6), $V_{\text{unc}} = 11 \mu\text{mol min}^{-1}$ per g tissue. For the catalyzed reaction, using Equation 7, with $E = 22 \times 10^{-6}$ M, we obtain:

$$V_{\text{cat}} = 6 \times 10^6 \text{ min}^{-1} \cdot 22 \times 10^{-6} \text{ M} \cdot 10^{-3} \text{ L} = 130,00 \mu\text{mol min}^{-1}. \quad 12.$$

⁶The values of Table 3 (63) have been criticized in a recent review (23) as "not necessarily correct" because outflow of Na^+ and Cl^- were not measured. This is not valid criticism, since the k_{in} values are calculated from initial rates. If outflow were a factor, the rates of Table 3 would be an underestimation, and HCO_3^- concentration in new fluid would be even greater than the 62 mM calculated.

We discarded the measured value of 245 mM for nascent HCO_3^- as an artifact of isotope exchange (63). It was never put forward to determine HCO_3^- accession, as claimed in (23). Nascent HCO_3^- is about 62 mM (Table 3).

Table 3 The accession rates of ions from plasma to CSF in the cat. Effect of carbonic anhydrase inhibition (CAI) (63)^a

		1 Plasma (mM)	2 k_{in}^b (min ⁻¹)	3 Accession Rate Col. 1 × Col. 2 (mM min ⁻¹)	4 Calc. in New Fluid ^c (mM)	5 Measured CSF conc. (mM)
Na ⁺	normal	147	0.016	2.4	164	158
	CAI		0.0076	1.1	157	
Cl ⁻	normal	115	0.013	1.5	104	134
	CAI		0.0073	0.8	112	
HCO ₃ ⁻	normal					
	as CO ₂	0.95	0.94	0.9 ^d	62 ^d	22
	as HCO ₃ ⁻	20	0.044			
	CAI					
	as CO ₂	0.95	0.29	0.3 ^d	42	
	as HCO ₃ ⁻	20	0.014			

^aFollowing 50 mg kg⁻¹ acetazolamide or 30 mg kg⁻¹ methazolamide i.v.^bRate of isotope delivery to CSF ÷ counts in plasma.^cCol. 3 × fluid turnover time. The latter is given by the ventricular volume (1.4 ml) divided by the rate of CSF flow (0.020 ml min⁻¹) = 70 min. When carbonic anhydrase is inhibited the volume is unchanged and rate of formation is halved, whence fluid turnover time = 140 min. See equation of Table 2.^dCalculated from Na⁺ minus Cl⁻ entrance (63). The movement of ¹⁴C species was complicated by isotope exchange yielding inaccurate values. See footnote 5.

The calculated and observed rates are compared in Table 4. Note that V_{unc} agrees well with V_{inh} , as in the examples given above for PJ and AH. The calculated V_{cat} , however, exceeds the observed catalytic rate by about 8000-fold. This ratio is considerably higher than for PJ and AH (see above) since the enzyme concentration in choroid plexus is unusually high, exceeding even kidney and equal to CA II in red cells (30). The result of this, predictably and borne out experimentally, is that the catalytic rate must be reduced nearly 10,000-fold (fractional inhibition = 0.9999) for pharmacological effect. Thus, 30 mg kg⁻¹ methazolamide is required for the CSF effect (60), but only 4 mg kg⁻¹ for AH (66).

Table 4 suggests that all of HCO₃⁻ entrance can be accounted for by the hydroxylation of CO₂, catalyzed and uncatalyzed, but the question remains whether any component of flow lies outside the dependence on this reaction. Recent experiments suggest that the uncatalyzed reaction is susceptible to inhibition, so that the total CO₂ contribution can be measured (61, 62). The CSF was perfused with various acids (AlCl₃, GaCl₃, acetic, phosphoric, hydrochloric, at pH 4.7). CSF flow decreased to some 67% of control rates.

Table 4 Calculated and observed rates of HCO_3^- formation in CSF of cat

Calculated ^{a,b}		Observed ^{a,c}	
		$V_{\text{total}} =$	24
$V_{\text{uncat}} =$	11	$V_{\text{inhib}} =$	8
V_{cat}	130,000	$V_{\text{cat}} =$	16 ($V_{\text{total}} - V_{\text{inhib}}$)

^a $\mu\text{mol min}^{-1}$ per g choroid plexus
^bSee text.
^cFrom Table 3, Col. 3, converting mM min^{-1} to $\mu\text{mol min}^{-1}$ per g choroid plexus using 1.4 ml as CSF volume, and choroid plexus weight = 50 mg.

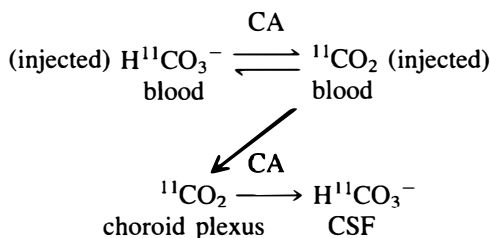
We attribute this to reduction of the uncatalyzed reaction to near zero, which would occur if pH were decreased one unit at the secretory site (Equation 2). Since the calculated uncatalyzed rate (using pH 9) agrees with the observed inhibited rate (Table 4), at pH 8 or less the observed uncatalyzed rate should be nearly abolished. CA inhibition causes a 42% decrease in flow, not greatly different from the effect on sodium accession (Table 3). Thus the uncatalyzed reaction contributes 33%, the catalyzed 42%, both dependent on HCO_3^- synthesis: 25% lies outside the CO_2 system, probably involving chloride (62).⁷

Thus while normal HCO_3^- accession is but 37% that of Na^+ (Table 3, the rest being Cl^-), this $\text{Na}^+ \text{-HCO}_3^-$ linked moiety controls 75% of flow. This emphasizes the special relation between HCO_3^- synthesis and movement, and fluid flow.

An analysis of the rates of HCO_3^- entrance to CSF under conditions of changing plasma HCO_3^- and P_{CO_2} led to the conclusion that the major factor in HCO_3^- accession is the catalytic conversion of $\text{CO}_2 \rightarrow \text{HCO}_3^-$ in choroid plexus (33). When CA is inhibited, HCO_3^- rises in choroid cells (21). This reflects an alkaline disequilibrium, i.e. OH^- is elevated when buffering by CO_2 is slowed.

The power of choroid plexus CA was shown by injecting $^{11}\text{CO}_2$ or $\text{H}^{11}\text{CO}_3^-$ intravenously in dogs; 80% of the label of either species entered the brain in a single pass (22). This fine experiment demonstrates rapid interconversion of the species in blood and choroid plexus as follows:

⁷ Our earlier work with AlCl_3 and GaCl_3 led to the incorrect conclusion that both catalyzed and uncatalyzed reactions were affected by these Lewis acids (61). A more recent study shows that the acids affect only the uncatalyzed reactions (62).



The catalytic power of the enzyme is so great that given the proper buffering and the unlimited source of CO₂, the gas can form any amount of HCO₃⁻ for transport. When the enzyme was inhibited systemically, first pass entry of ¹¹C from CO₂ was reduced to 50% and of ¹¹C from HCO₃⁻ to 20%. Even in the uncatalyzed situation, the reaction gives one third the normal rate (Table 3).

The CSF-plasma transepithelial P.D. is dependent on plasma pH: in the dog, at pH 7.4, P.D. = 3–4 mV, CSF positive (2, 11). Acetazolamide increased P.D. about 1 mV (11), the same direction and magnitude reported for CA inhibition in AH (25). pH homeostasis in CSF does not result from the P.D. (2), but from HCO₃⁻ movement. The critical effect of CA inhibition appears to be to lower the ratio Δ P.D./Δ pH (11); this agrees with the role of the enzyme in maintaining a high HCO₃⁻ gradient from cell to CSF, and that the inhibitor reduces the gradient. The results are consistent with the P.D. in both AH and CSF being a HCO₃⁻ diffusion potential.

Alligator Kidney

Alligator mississippiensis and related species normally excrete alkaline (pH 7.8) urine with about 60–80 meq L⁻¹ of NH₄⁺ and HCO₃⁻. Na⁺ and Cl⁻ are virtually absent. Clearly an efficient system is at work for formation of both ions. NH₄⁺ is made by deamination of amino acids, chiefly glycine and alanine. HCO₃⁻ is made from CO₂ + OH⁻ as described for PJ, AH, and CSF. The kidney excretes some 20% of metabolic CO₂ as HCO₃⁻. When acetazolamide is given, urinary HCO₃⁻ and pH drop to 5 meq L⁻¹ and 7.0 respectively, Cl⁻ increases 30-fold to about 90 meq L⁻¹, and NH₄⁺ is somewhat increased, due to increased urinary acid. HCO₃⁻ excretion appears to subserve fluid excretion and Cl⁻ conservation; this is a clear case of HCO₃⁻-Cl⁻ exchange. The alligator physiologists believe that the role of renal CA is mainly to conserve Cl⁻ (10).

HCO₃⁻ and CO₃²⁻ SYNTHESIS TO PROVIDE HIGH pH

Alkaline Gland of Skate

Males of the genus *Raja* (or skates) contain small paired sacs on the ventral aspect of the genitourinary system which empty (along with urinary ducts)

into the urinary papilla. The glands are highly vascular with simple columnar epithelium and brush border. Depending on the species and size of the fish, the gland contains 1–10 ml of clear fluid. In two species (*Raja ocellata* and *Raja erinacea*) the pH is 9.2 and total CO_2 is 212 mM. From the pKs of the proton dissociation of H_2CO_3 , it may be calculated that this total is divided about equally between HCO_3^- . This is the most alkaline fluid recorded for the vertebrate world. The anatomy of the gland and ionic composition of the fluids are given in the original paper (37).

In these two species the gland contains CA, and when fish were treated with methazolamide, the total CO_2 concentration was somewhat reduced. This suggests that the catalytic hydroxylation of CO_2 forms CO_3^{2-} as well as HCO_3^- . Of particular interest was the finding that a third species *Raja stabuliformis*, has alkaline glands of the same type, but the total CO_2 concentration is only 100 mM and the pH is less than that in the other 2 species, about 8.7. There is no CA in glands of *R. stabuliformis*. Nature has kindly furnished an example of the uncatalyzed reaction at work, with parallel data for the catalyzed reaction in the other two species (37).

The transcellular P.D. is about 7 mV, lumen negative to serosa, and the apical P.D. is -41 mV, cell negative (52). Thus HCO_3^- formed within the cell could diffuse down its electrochemical gradient (to 200 mM in lumen) if cellular concentration were maintained by its synthesis at 40 mM, which is not an impossible value. Chloride secretion accounts for the entire short circuit current, indicating a parallel to Na^+ - K^+ coupled Cl^- transport in the intestine and ascending loop of Henle. The alkalization process was considered electrically silent—perhaps a close linkage with Na^+ . Sadly the effect of CA inhibitors on the electrical properties of the system was not studied.

Rectal Salt Gland of Mosquito Larva

Larva of *Aedes dorsalis* inhabit lakes of extremely alkaline saline environments, with pH to 10.5, HCO_3^- to 250 mM, and CO_3^{2-} to 100 mM. Isolated rectal salt glands of these larva secrete total CO_2 at very high rates against a transepithelial potential of -31 mV, lumen negative (56).

Using refined microperfusion techniques for net chemical flux measurements and electrical studies of the isolated gland, it was shown that serosal addition of acetazolamide, or CO_2 removal, inhibited total CO_2 accumulation by about 80% (Figure 2). There was a marked decrease of the transepithelial P.D., with hyperpolarization of the apical membrane (Figure 2), but no effect on the basolateral membrane (54, 55). These and other experiments suggest that $\text{CO}_2/\text{HCO}_3^-$ enters the cell via a basolateral electroneutral mechanism for Cl^- . $\text{HCO}_3^-/\text{CO}_3^{2-}$ is formed in the cell as shown in Figure 2. Exit to lumen is through an electrogenic HCO_3^- or H^+ carrier (54, 55). Although not stressed, it is clear that a key event in $\text{HCO}_3^-/\text{CO}_3^{2-}$ secretion is their catalytic formation, linked to high apical permeability.

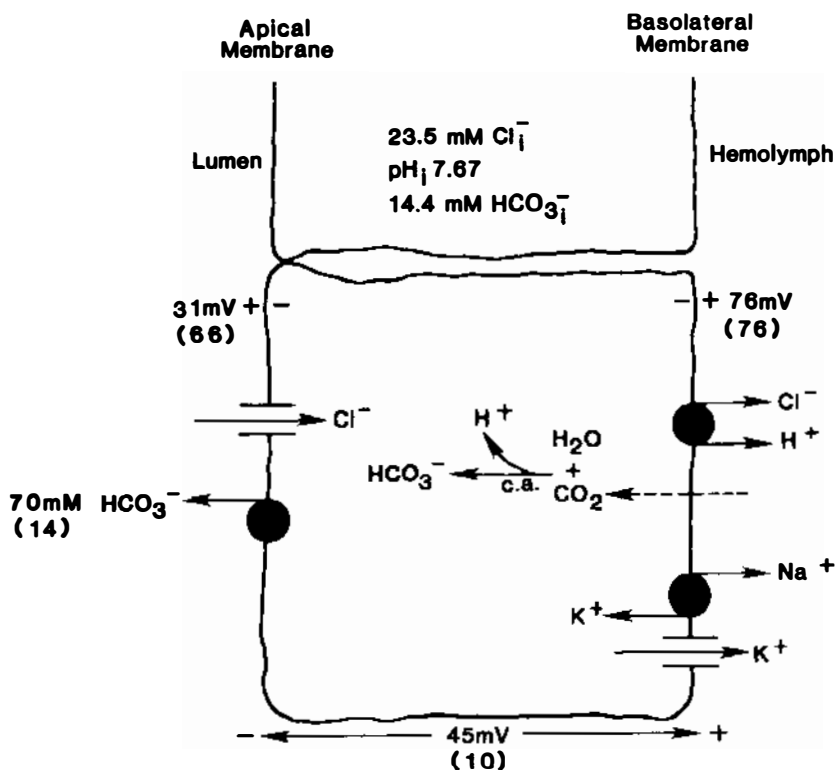


Figure 2 Model proposed for HCO₃⁻ transfer in the rectal gland of mosquito larva (48). Values in parentheses are those following complete carbonic anhydrase inhibition.

Gastro-Duodenal Alkalinization

Surface mucosal epithelial cells of the amphibian and mammalian gastric fundus and antrum secrete HCO₃⁻. Duodenal mucosa has the same function. These cells contain CA (28). The purpose appears to be protection of the mucosa against parietal cell acid secretion; indeed when the pH of bulk secretion is 1–2, the surface mucus gel maintains a pH of 7 (15). Addition of 10⁻⁴ M acetazolamide to the luminal side of isolated non-acid secreting fundi of *Rana temporaria* reduced HCO₃⁻ secretion to 30% of normal. There was no effect on P.D. or resistance (15).

These observations explain an older finding (then appearing paradoxical since CA inhibition reduces acid secretion and has been used to treat ulcers), namely that acetazolamide causes ulcers in dogs, when H⁺ concentration of the stomach lumen is raised to 30 mM (65). Thus inhibition of alkalinization decreases the ability of the stomach to resist low pH, even though endogenous acid production may be reduced. There is the suggestion that surface mucosal

alkalinization is more sensitive to CA inhibition than parietal cell acidification (15); the basis for this may be higher concentration of CA at the latter site. An excellent review is available (16).

RELATION OF HCO_3^- TO H^+ SECRETION

H^+ secretion is not considered here, but it is important to mention that it is, chemically, part of the same process as HCO_3^- secretion (Figure 1). In the two chief organs of H^+ secretion, kidney and stomach (parietal cell), HCO_3^- is returned to the blood. In kidney, details of this process have been worked out beautifully as described in the introduction (4, 6). In the stomach, the enormous magnitude of H^+ secretion is reflected in the "alkaline tide" of the blood, as recognized for many years.

Renal acidification and HCO_3^- reabsorption have been covered in a fine monograph, which points out: (a) Proximal HCO_3^- reabsorption is 80–90% dependent on CA. For these high rates, the uncatalyzed reaction is negligible. (b) Distal H^+ secretion is dependent on CA. (c) When the enzyme is inhibited, new high HCO_3^- gradients from lumen to blood are developed distally, since proximal HCO_3^- (but not H_2O) reabsorption is greatly reduced. Thus distal HCO_3^- back diffusion becomes dominant, and only about 25% of filtered HCO_3^- appears in the urine (1).

The CO_2 -CA system in the parietal cell has been neglected recently. I reviewed the large literature on the subject 20 years ago (30) and short texts giving a unified scheme are presently available (49). The particular issue of whether CO_2 can be dissociated from H^+ secretion has been answered in the affirmative (9, 43), in agreement with our finding in the elasmobranch kidney (59). In the 1987 Annual Review of Physiology a chapter is devoted to the pH of the parietal cell, with some reference to CO_2 (see footnote 3).

HCO_3^- SYNTHESIS SUBSERVING EXCRETION OF CO_2 ("FACILITATED DIFFUSION")

In this section, I consider three organs in which neither H^+ nor HCO_3^- are excreted. The high concentration of CA and the effect of inhibition were puzzling for many years (30), but now have been clarified.

Lens

Mammalian, avian and amphibian lenses all have CA, but elasmobranch fish do not (30). This, combined with inhibition studies, provided an unusual opportunity to study function.

Inhibition studies were carried out on rabbit lens in vivo and in vitro, with care taken to use sulfonamides that permeate the lens. There was no effect on

fluxes of K⁺ (as Rb⁺), Na⁺, or Cl⁻. Measured and calculated potentials suggest high K⁺ permeability in the tissue (19). The effect of the inhibitors appeared solely to increase total CO₂ in the lens, from 33 to 66 mmol kg⁻¹ (in vivo) and from 28 to 40 mmol kg⁻² (in vitro). The elasmobranch lens, containing no CA, normally has total CO₂ 4 times greater than the surrounding AH, in contrast to the rabbit where the concentration in lens is only about 12% higher (17).

From the metabolic rates and geometry of rabbit lens, it was calculated that, based on CO₂ diffusion alone, a gradient of at least 25 mm Hg would be necessary to carry off CO₂. Compared to diffusion rates, the uncatalyzed interconversion of HCO₃⁻ ⇌ CO₂ is negligible. The catalytic rates, however, exceed the CO₂ diffusion threefold.

It was concluded that, in this avascular tissue of radius 0.5 cm, CO₂ diffusion requires large gradients, as seen in the fish and the inhibited lens. Elimination of CO₂ is normally carried out by its interconversion to HCO₃⁻, as diagramed in Figure 3 (17).

Rectal Gland of Elasmobranch

This gland is an appendix like structure attached to the intestine of elasmobranch fish. Under the stimulus of volume expansion or saline load (presumably mimicking sea water intake) the gland secretes (in a 2–4 kg fish) some 8–20 ml hr⁻¹ of 0.5 M NaCl, which is essentially its concentration in sea water (13).

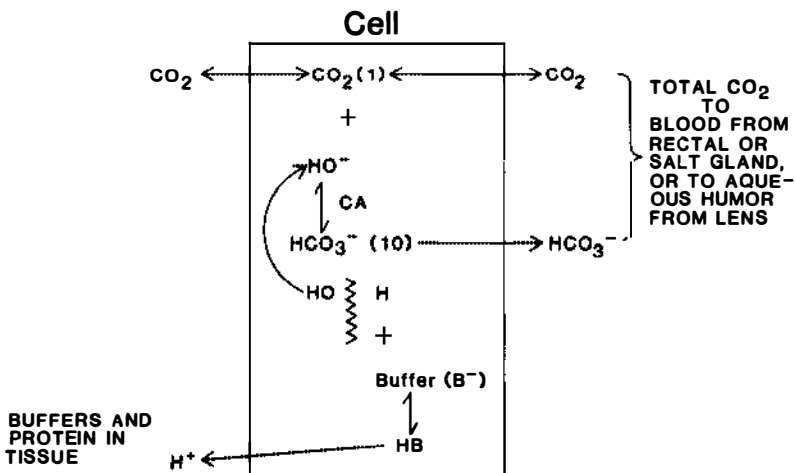


Figure 3 Model showing facilitated diffusion of gaseous CO₂, produced by the cell and converted to HCO₃⁻, thus increasing the gradient for diffusion out of elasmobranch rectal gland, avian salt gland, and lens. In parentheses are the equilibrium concentrations (mM) of the CO₂ species, presuming pH 7.1 in the cell.

The gland has a high concentration of CA (29), seemingly a mystery since the secretion is neutral. After some conflicting results, it was found that methazolamide, under the right conditions (notably high, well-controlled flow rates) reduced secretion by half. But there was no change in fluid composition; it was still 0.5 M NaCl and slightly acidic. The notable change was a four fold increase in P_{CO_2} and doubling of total CO_2 in gland fluid (58). It appeared that as for lens, metabolic CO_2 could not be carried off in normal fashion when CA is inhibited. (In the normal secreting gland, P_{CO_2} is not higher than in venous blood.) The gland has adequate vascularization, but when it secretes, CO_2 output rises 30-fold (50). In this special situation, catalytic $CO_2 \rightleftharpoons HCO_3^-$ interconversion seems necessary to maintain normal P_{CO_2} . The reason that CA inhibition lowers flow is that acidosis is inimical to secretion, as demonstrated by the similar effects of HCl and 5% CO_2 (58).

Avian Salt Gland

The functions of the salt or nasal gland in marine birds (46), like those of the rectal gland in elasmobranchs (7) and the alkaline gland of the skate (37), were discovered at the Mount Desert Island Biological Laboratory about 30 years ago.

As for the rectal gland, the avian gland secretion is turned on by the infusion of saline. Fluid is neutral, hypertonic to the blood and to the sea. The gland contains high concentrations of CA, and is extremely sensitive to inhibition. A full (16 mg kg^{-1}) dose of methazolamide cuts the saline stimulated flow (in sea gulls) from about 6 ml hr^{-1} to zero (40). This "complete effect" is unique; for other secretory systems inhibition cuts flow to 20–50% of normal. The effect of methazolamide and high CO_2 and HCl is to elicit acidosis, which as stated, is inimical to secretion. Metabolic and respiratory acidosis also reduce secretion (40). Thus it seems reasonable to assume, that as in the elasmobranch rectal gland the stimulated system yielding high CO_2 output requires catalytic conversion to HCO_3^- .

Literature Cited

- Alpern, R. J., Warnock, D. G., Rector, F. C. Jr. 1986. Renal acidification mechanisms. In *The Kidney*, ed. B. M. Brenner, F. C. Rector, Jr., 1:206–49. Philadelphia: Saunders. 3rd ed.
- 1a. Ammar, E. M., Hutson, D., Scratcherd, T. 1987. Absence of a relationship between arterial pH and pancreatic bicarbonate secretion in the isolated perfused cat pancreas. *J. Physiol. (London)* 388:495–504
- Bledsoe, S. W., Eng, D. Y., Hornbein, T. F. 1981. Evidence of active regulation of cerebrospinal fluid acid-base balance. *J. Appl. Physiol.* 51:369–75
- Buanes, T., Grotmol, T., Landsverk, T., Ridderstrale, Y., Raeder, M. G. 1986. Histochemical localization of carbonic anhydrase in the pig's exocrine pancreas. *Acta Physiol. Scand.* 128: 437–44
- Burckhardt, B.-Ch., Cassola, A. C., Frömter, E. 1984. Electrophysiological analysis of bicarbonate permeation across the peritubular cell membrane of rat kidney proximal tubule. II. Exclusion of HCO_3^- -effects on other ion permeabilities and of coupled electroneutral HCO_3^- -transport. *Pflüg. Arch.* 401:43–51

5. Burckhardt, B.-Ch., Geers, C., Frömter, E. 1985. Role of membrane-bound carbonic anhydrase in HCO₃⁻ transport across rat renal proximal tubular cell membranes. *Pflüg. Arch.* 405 (Suppl. 2):R31.
6. Burckhardt, B.-Ch., Sato, K., Frömter, E. 1984. Electrophysiological analysis of bicarbonate permeation across the peritubular cell membrane of rat kidney proximal tubule. I. Basic observations. *Pflüg. Arch.* 401:34-42.
7. Burger, J. W., Hess, W. N. 1960. Function of the rectal gland in the spiny dogfish. *Science* 131:670-71.
8. Case, R. M., Argent, B. E. 1986. Bicarbonate secretion by pancreatic duct cells: Mechanisms and control. In *The Exocrine Pancreas: Biology, Pathobiology, and Diseases*, ed. V. L. W. Go, J. D. Gardner, F. P. Brooks, E. Lebenthal, E. P. DiMagno, G. A. Scheele, pp. 213-43. New York: Raven.
9. Chacin-Meleán, J., Alonso, D., Harris, J. B. 1974. The influence of pH, buffer species and gas composition on acid secretion of frog gastric mucosa. In *Gastric Hydrogen Ion Secretion*, ed. D. K. Kasbekar, G. Sachs, W. S. Rehm 3:237-59. New York: Dekker.
10. Coulson, R. A., Hernandez, T. 1983. In *Alligator Metabolism*. New York: Pergamon.
11. Davies, D. G., Britton, S. L., Gurtner, G. H., Dutton, R. E., Krasney, J. A. 1984. Effect of carbonic anhydrase inhibition on the DC potential difference between cerebrospinal fluid and blood. *Expl. Neurol.* 86:66-72.
12. Dawson, H. 1967. *Physiology of the Cerebrospinal Fluid*, pp. 70-79, 124-26. London: Churchill.
13. Epstein, F. H., Stoff, J. S., Silva, P. 1983. Mechanism and control of hyperosmotic NaCl-rich secretion by the rectal gland of *Squalus acanthias*. *J. Exp. Biol.* 106:25-41.
14. Faurholt, C. 1924. Etudes sur les solutions aqueuses d'anhydride carbonique et d'acide carbonique. *J. Chim. Phys.* 21:400-55.
15. Flemström, G. 1977. Active alkalization by amphibian gastric fundic mucosa in vitro. *Am. J. Physiol.* 233:E1-12.
16. Flemström, G. 1987. Gastric and duodenal mucosal bicarbonate secretion. In *Physiology of the Gastrointestinal Tract*, ed. L. K. Johnson 2:1011-30. New York: Raven.
17. Friedland, B. R., Maren, T. H. 1981. The relation between carbonic anhydrase activity and ion transport in elasmobranch and rabbit lens. *Exp. Eye Res.* 33:545-61.
18. Grassl, S. M., Holohan, P. D., Ross, C. R. 1987. HCO₃⁻ transport in basolateral membrane vesicles isolated from rat renal cortex. *J. Biol. Chem.* 262:2682-27.
19. Green, K., Bountra, C., Georgiou, P., House, C. R. 1985. An electrophysiologic study of rabbit ciliary epithelium. *Invest Ophthalmol. Visual Sci.* 26:371-81.
20. Henriques, O. M. 1928. Über die geschwindigkeiten der anhydrirung bzw. der hydratisierung der kohlen saurekomponenten im blute. *Biochem. Z.* 200:1-5.
- 20a. Iijima, T., Yamagishi, T., Iwatsuki, K., Chila, S. 1976. Effects of arterial pH and HCO₃⁻ concentration on HCO₃⁻ secretion in the isolated blood perfused dog pancreas. *Arch. Int. Pharmacol.* 279:314-23.
21. Johansen, C. E. 1984. Differential effects of acetazolamide, benzolamide and systemic acidosis on hydrogen and bicarbonate gradients across the apical and basolateral membranes of the choroid plexus. *J. Pharmacol. Exp. Ther.* 231:502-11.
22. Johnson, D. C., Hoop, B., Kazemi, H. 1983. Movement of CO₂ and HCO₃⁻ from blood to brain in dogs. *J. Appl. Physiol.* 54:989-96.
23. Kazemi, H., Johnson, D. C. 1986. Regulation of cerebrospinal fluid acid-base balance. *Physiol. Rev.* 66:953-1037.
24. Khalifah, R. G. 1971. The carbon dioxide hydration activity of carbonic anhydrase. Stop-flow kinetic studies on the native human isoenzymes B and C. *J. Biol. Chem.* 246:2561-73.
25. Kishida, K., Miwa, Y., Iwata, C. 1986. 2-substituted 1,3,4-thiadiazole-5-sulfonamides as carbonic anhydrase inhibitors: Their effects on the transepithelial potential difference of the isolated rabbit ciliary body and on the intraocular pressure of the living rabbit eye. *Exp. Eye Res.* 43:981-95.
26. Kuipers, G. A. J., Van Nooy, I. G. P., De Pont, J. J. H. M., Bonting, S. L. 1984. Anion secretion by the isolated rabbit pancreas. *Biochim. Biophys. Acta* 774:269-76.
27. Kuipers, G. A. J., Van Nooy, I. G. P., De Pont, J. J. H. M., Bonting, S. L. 1984. The mechanism of fluid secretion in the rabbit pancreas studied by means of various inhibitors. *Biochim. Biophys. Acta* 778:324-31.
28. Lonnerholm, G. 1977. Carbonic anhydrase in the intestinal tract of the guinea pig. *Acta Physiol. Scand.* 99:53-61.
29. Maren, T. H. 1962. Ionic composition

- of cerebrospinal fluid and aqueous humor of the dogfish, *Squalus acanthias*. II. Carbonic anhydrase activity and inhibition. *Comp. Biochem. Physiol.* 5:201-15
30. Maren, T. H. 1967. Carbonic anhydrase: Chemistry, physiology, and inhibition. *Physiol. Rev.* 47:595-781.
 31. Maren, T. H. (with the technical assistance of Kent, B. B., Welliver, R. C. Woodworth, R. B.). 1972. Bicarbonate formation in cerebrospinal fluid: Role in sodium transport and pH regulation. *Am. J. Physiol.* 222:885-99.
 32. Maren, T. H. 1979. An historical account of CO₂ chemistry and the development of carbonic anhydrase inhibitors. The 1979 Theodore Weicker Memorial Award Oration. *Pharmacologist* 20:303-21.
 33. Maren, T. H. 1979. Effect of varying CO₂ equilibria on rates of HCO₃⁻ formation in cerebrospinal fluid. *J. Appl. Physiol.* 41:471-77
 34. Maren, T. H. 1984. A general view of HCO₃⁻ transport processes in relation to the physiology and biochemistry of carbonic anhydrase. In *Secretion: Mechanisms and Control*, ed. R. M. Case, J. M. Lingard, J. A. Young, pp. 47-66. Manchester: Manchester Univ. Press
 35. Maren, T. H. 1984. The development of ideas concerning the role of carbonic anhydrase in the secretion of aqueous humor: Relation to the treatment of glaucoma. In *Glaucoma: Applied Pharmacology in Medical Treatment*, ed. S. M. Drance, A. H. Neufeld, pp. 325-55. Orlando, FL: Grune and Stratton
 36. Maren, T. H., Haywood, J. R., Chapman, S. K., Zimmerman, T. J. 1977. The pharmacology of methazolamide in relation to the treatment of glaucoma. *Invest. Ophthalmol. Visual Sci.* 16:730-42.
 37. Maren, T. H., Rawls, J. A., Burger, J. W., Myers, A. C. 1963. The alkaline (Marshall's) gland of the skate. *Comp. Biochem. Physiol.* 10:1-16.
 38. Meldrum, N. U., Roughton, F. J. W. 1933. Carbonic anhydrase: Its preparation and properties. *J. Physiol. (London)* 80:113-42.
 39. Mitchell, P. 1985. The correlation of chemical and osmotic forces in biochemistry. *J. Biochem.* 97:1-18
 40. Nechay, B. R., Larimer, J. L., Maren, T. H. 1960. Effects of drugs and physiologic alterations on nasal salt excretion in sea gulls. *J. Pharmacol. Exp. Ther.* 130:401-10
 41. Raeder, M., Mathisen, O. 1982. Abolished relationship between pancreatic HCO₃⁻ secretion and arterial pH during carbonic anhydrase inhibition. *Acta Physiol. Scand.* 114:97-102
 42. Rawls, J. A., Wistrand, P. J., Maren, T. H. 1963. Effects of acidbase changes and carbonic anhydrase inhibition on pancreatic secretion. *Am. J. Physiol.* 205:651-57
 43. Sanders, S. S., Hayne, V. B. Jr., Rehm, W. S. 1973. Normal H⁺ rates in frog stomach in absence of exogenous CO₂ and a note on pH stat method. *Am. J. Physiol.* 225:1311-21
 44. Sanyal, G., Maren, T. H. 1981. Thermodynamics of carbonic anhydrase catalysis. A comparison between human isoenzymes B and C. *J. Biol. Chem.* 256:608-12
 45. Sasaki, S., Shigai, T., Yoshiyama, N., Takeuchi, J. 1987. Mechanism of bicarbonate exit across basolateral membrane of rabbit proximal straight tubule. *Am. J. Physiol.* 252(21):F11-18
 46. Schmidt-Nielsen, K., Jorgensen, G. C., Osaki, H. 1958. Extrarenal salt excretion in birds. *Am. J. Physiol.* 193-101-7
 47. Schulz, I., Strover, F., Ullrich, K. J. 1971. Lipid soluble weak organic acid buffers as "substrate" for pancreatic secretion. *Pflug. Arch.* 323:121-40
 48. Schulz, I., Terreros-Aranguren, D. 1982. Sidedness of transport steps involved in pancreatic HCO₃⁻ secretion. In *Electrolyte & Water Transport Across Gastrointestinal Epithelia*, ed. R. M. Case, A. Garner, L. A. Turnberg, J. A. Young, pp. 143-56. New York: Raven
 49. Sernka, T., Jacobson, E. 1979. *Gastrointestinal Physiology*. Baltimore, MD: Williams & Wilkins
 50. Silva, P., Stoff, J. S., Solomon, R. J., Rosa, R., Stevens, A., et al. 1980. Oxygen cost of chloride transport in perfused rectal gland of *Squalus acanthias*. *J. Membr. Biol.* 53:215-21.
 51. Sirs, J. A. 1958. Electrometric stopped flow measurements of rapid reactions in solution. Part II. Glass electrode pH measurements. *Trans. Faraday Soc.* 54:207-12
 52. Smith, P. L. 1985. Electrolyte transport by alkaline gland of little skate *Raja erinacea*. *Am. J. Physiol.* 248(17):R346-52
 53. Soleimani, M., Grassl, S. M., Aronson, P. S. 1987. Stoichiometry of Na⁺-HCO₃⁻ cotransport in basolateral membrane vesicles isolated from rabbit renal cortex. *J. Clin. Invest.* 79:1276-80
 54. Strange, K., Phillips, J. E. 1984. Mechanisms of CO₂ transport in rectal salt gland of *Aedes*. I. Ionic requirements of CO₂ secretion. *Am. J. Physiol.* 246(15):R727-34

55. Strange, K., Phillips, J. E. 1985. Cellular mechanism of HCO₃⁻ and Cl⁻ transport in insect salt gland. *J. Membr. Biol.* 83:25-37
56. Strange, K., Phillips, J. E., Quamme, G. A. 1982. Active HCO₃⁻ secretion in the rectal salt gland of a mosquito larva inhabiting NaHCO₃-CO₃ lakes. *J. Exp. Biol.* 101:171-86.
57. Swanson, C. H., Solomon, A. K. 1975. Micropuncture analysis of the cellular mechanisms of electrolyte secretion by the in vitro rabbit pancreas. *J. Gen. Physiol.* 65:22-45
58. Swenson, E. R., Maren, T. H. 1984. Effects of acidosis and carbonic anhydrase inhibition in the elasmobranch rectal gland. *Am. J. Physiol.* 247(16): F86-92
59. Swenson, E. R., Maren, T. H. 1986. Dissociation of CO₂ hydration and renal acid secretion in the dogfish, *Squalus acanthias*. *Am. J. Physiol.* 250(19): F288-93
60. Vogh, B. P. 1980. The relation of choroid plexus carbonic anhydrase activity to cerebrospinal fluid formation: Study of three inhibitors in cat with extrapolation to man. *J. Pharmacol. Exp. Ther.* 213: 321-31.
61. Vogh, B. P., Godman, D. R., Maren, T. H. 1985. Aluminum and gallium arrest formation of cerebrospinal fluid by the mechanism of OH⁻ depletion. *J. Pharmacol. Exp. Ther.* 233:715-21
62. Vogh, B. P., Godman, D. R., Maren, T. H. 1987. The effect of AlCl₃ and other acids on cerebrospinal fluid production: A correction. *J. Pharmacol. Exp. Ther.* 242:35-39
63. Vogh, B. P., Maren, T. H., 1975. Sodium, chloride, and bicarbonate movement from plasma to cerebrospinal fluid in cats. *Am. J. Physiol.* 228:673-83
64. Way, L. W., Diamond, J. M. 1970. The effect of secretin on electrical potential differences in the pancreatic duct. *Biochim. Biophys. Acta* 203:298-307
65. Werther, J., Hollander, F., Altamirano, M. 1965. Effect of acetazolamide on gastric mucosa in canine vivo-vitro preparations. *Am. J. Physiol.* 209:127-33
66. Wistrand, P. J., Rawls, J. A. Jr., Maren, T. H. 1961. Sulfonamide carbonic anhydrase inhibitors and intraocular pressure in rabbits. *Acta Pharmacol. Toxicol.* 5:193-200.
67. Yoshitomi, K., Burckhardt, B.-Ch., Frömter, E. 1985. Rheogenic sodium-bicarbonate cotransport in the peritubular cell membrane of rat renal proximal tubule. *Pflüg. Arch.* 405:360-66